Influence of prostatic blood flow on laser prostatectomy

van Swol, Christiaan, Verdaasdonck, Rudolf, Mooibroek, Jaap, Boon, Tom

Christiaan F. P. van Swol, Rudolf M. Verdaasdonck, Jaap Mooibroek, Tom A. Boon, "Influence of prostatic blood flow on laser prostatectomy," Proc. SPIE 2129, Lasers in Urology, (2 May 1994); doi: 10.1117/12.175017

SPIE.

Event: OE/LASE '94, 1994, Los Angeles, CA, United States

Influence of prostatic blood flow on laser prostatectomy

Christiaan F.P. van Swol[1,2], Rudolf M. Verdaasdonk[1], Jaap Mooibroek[3] and Tom A. Boon[2]

Medical Laser Center[1], Depts. of Urology[2] and Radiotherapy[3],
University Hospital Utrecht, Utrecht, The Netherlands

ABSTRACT

Normally, a laser prostatectomy to treat Benign Prostatic Hyperplasia (BPH) is performed using a fixed dosimetry. Differences in, e.g., blood flow, optical properties and geometry, are not taken into account, although most of these differences may be distinguished when performing a cystoscopy, e.g., the color of the prostate. These characteristics show their influence in the final tissue effect. We developed a model to predict the permanent damage to the tissue.
A Monte Carlo simulation program was used to calculate the light distribution in the prostate due to Nd:YAG laser light irradiation. Consequently, using the absorbed energy as a heat source, the thermal distribution in the tissue was computed using the method of finite differences. This numerical model was combined with a rate process damage model (Henriques equation) to make it possible to predict the extent of laser induced permanent damage (denaturation). The model is dynamic in time, which enabled us to observe the evolution of the damage process. In this flexible model blood vessels were incorporated.
The blood vessels showed to have major influence on the temperature distribution and on the created damage. The vessels act like a heat sink, which clamps the temperature and shields the heat to penetrate deep into the tissue

1. INTRODUCTION

The use of the Nd:YAG laser for the transurethral treatment of Benign Prostatic Hyperplasia (BPH) has been introduced into medical practice in 1991,[1,2] after initial experience in a canine model.[3,4,5] Since then, at least six devices have been developed to bring laser light in a proper way into the prostatic area. All devices are modifications of a bare optical fiber. The light coming out of a fiber is deflected off axis in order to deliver the light to the prostatic tissue surrounding the urethra. The dosimetry protocols used for application of the devices differ, but they have in common that individual prostate characteristics, like, blood flow, optical properties and geometry, are usually not taken into account. Most of these characteristics can be appreciated when performing a pre-operative cystoscopy.
In this study, the influence of different parameters such as the local irradiation time and blood perfusion is evaluated, using a numerical model to calculate and to visualize the dynamic temperature distribution and the tissue necrosis in the prostate, induced by transurethrally delivered Nd:YAG laser light. The temperature distribution in the prostate and the therapeutic effect of a laser induced prostatectomy are presented graphically.

2. MATERIALS AND METHODS

2.1. Numerical Model

The numerical model[6] consists of three parts: an optical, a thermal and a tissue response part. The light distribution was computed using a Monte Carlo simulation program.[7] As input for the Monte Carlo program the optical parameters for prostatic tissue at 1064 nm were used[8]: μ_a=0.37 cm^{-1} and μ'_s=8.2 cm^{-1}. Using the light distribution, the generated heat due to absorption was calculated. Consequently, the dynamic temperature distribution in the tissue

0-8194-1422-0/94/$6.00

was calculated using the method of finite differences.[9] The thermal properties of the tissue used, are: $C_{p,tissue}$=3600 $J.Kg^{-1}.K^{-1}$ and k_{tissue}=0.5 $W.m^{-1}$. The optical and thermal parameters were assumed to be independent of temperature. The results of the temperature calculations were combined with a rate process damage model, that made it possible to predict the extent of the laser induced thermal damage (tissue necrosis). The damage function Ω, derived from the Arrhenius equation[10], is described by:

$$\Omega(r,t) = A\int_0^t e^{\left(\frac{-\Delta E}{R.T(r,t)}\right)} dt \qquad (1)$$

where A is a pre-exponential constant (s^{-1}), ΔE is the activation energy ($cal.mol^{-1}$), R is the universal gas constant (2 $cal.mol.K^{-1}$) and T(r,t) is the previously calculated place and time dependent temperature distribution (K). The values used were: A= 1.67 10^{13} s^{-1} and E= 23,000 $cal.mol^{-1}$. As long as Ω does not exceed the value of 1 the damage done to the tissue is reversible. If Ω exceeds 1 the damage has become irreversible and hence the tissue is permanently damaged.

In the numerical model, the geometry was assumed to be planar and the dimensions were chosen to simulate the clinical situation as much as possible (see figure 1).

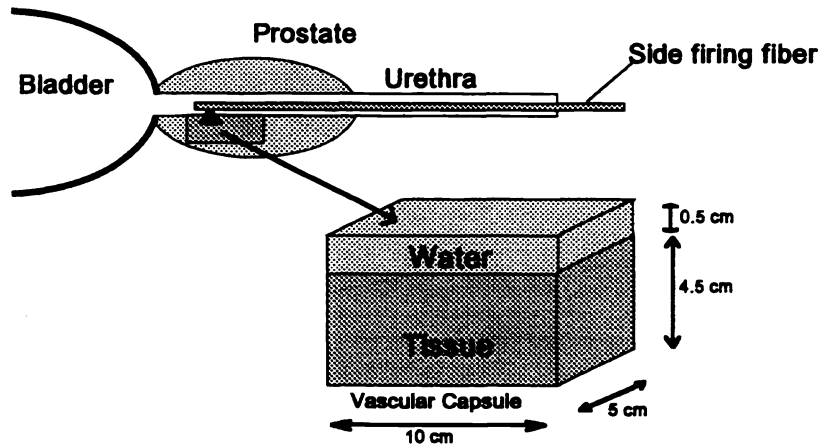

Figure 1. Dimensions and geometry of the phantom model.

The urethra was represented by a five millimeter layer of water on top of the tissue. As boundary conditions, the planes at the side of the bladder, the vascular capsule and the urethra were assumed isothermal, the other planes were assumed adiabatic. The diameter of the gaussian beam used was 3 mm at the water/tissue interface.

2.2. Arterial and venous network

A network of arterial and venous vessels was incorporated in the prostate model (figure 2). The arteries were positioned in a plane 2 mm beneath the surface (representing the urethral wall) and the veins were positioned 2 mm lower. Both networks had the same geometrical shape. The diameter of all the vessels was 1 mm, the initial blood flow was 10 cm/s and the arterial and the venous flow were counter current. As the diameter of all the vessels is the same the blood flow is equally divided at each side branch. To evaluate the effect of perfusion, the blood vessels were only present in the left half of the model.

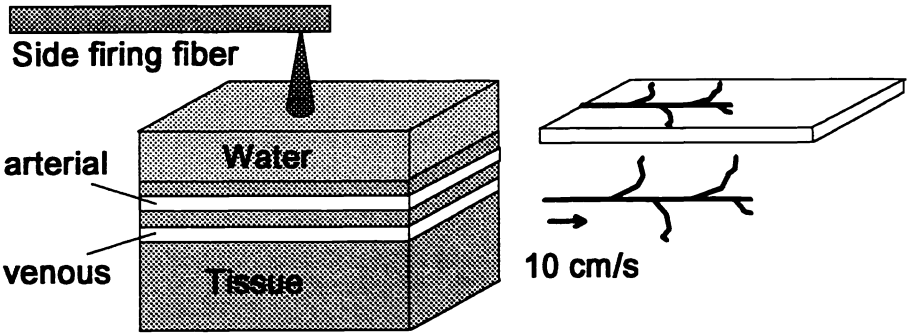

Figure 2. Position of the arterial and venous network in the model, the blood vessels are only positioned in the left half of the model.

2.3 Methods of application

After a side fire laser fiber has been inserted in the prostatic urethra, the energy can be applied to the tissue in two different ways: static or moving. In the case of a static application the fiber is positioned at a certain place and remains there for a fixed amount of time, while irradiating the tissue with a pre-defined power. The irradiation time and power depend on the protocol, that is prescribed by the manufacturer. In the case of a moving application, the fiber is positioned at a certain place and then during irradiation slowly moved (scanned) over the tissue with a pre-defined power. Again the irradiation time, power, scanning speed and scanning direction depend on the protocol used. Both application methods are incorporated in the model. For the moving application the scanning speed was varied.

3. RESULTS

3.1. Graphical representation of the calculated results

The calculations provided, at every time step, a three dimensional array from which either a transversal or an axial plane was taken for graphical representation (see figure 3).

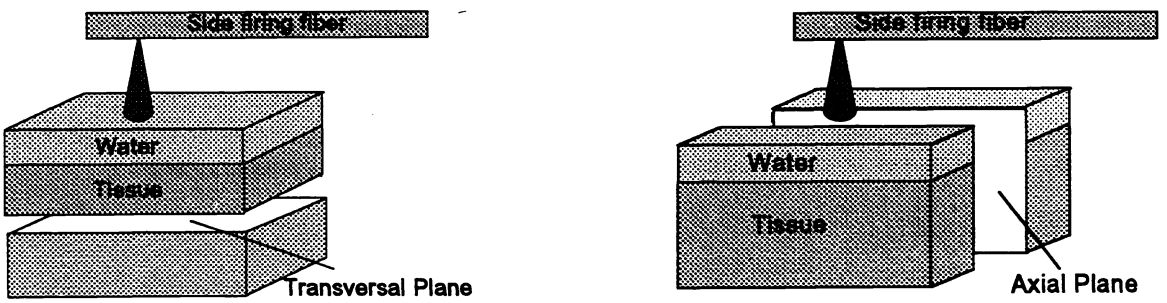

Figure 3. The calculated three dimensional temperature distribution in the phantom model is graphically presented as a plane, either transversal (left) or axial (right).

The axial planes presented here are slices through the middle of the tissue model (figure3, right). The transversal planes are slices at 1 mm under the water/tissue interface (figure 3, left). The calculated temperatures were displayed as gray shades from dark gray, representing ambient temperature to light gray, representing a 60 degrees temperature

rise from body temperature. White represents a temperature rise exceeding the boiling point of water at 100 degrees. The gray scale is linear. The size of each frame is 5x10 cm (see figure 1). Every temperature frame is coupled to a tissue necrosis frame, which represents the extent of permanent damage. Either the tissue is permanently damaged ($\Omega > 1$), represented by white, or not damaged ($\Omega < 1$), represented by black.

3.2. Influence of blood flow and method of application on laser induced damage

The results are discussed for the two different methods of application: a moving laser beam, scanning the surface of the prostate, and a static laser beam, remaining at one position above the prostatic tissue. In both cases the influence of prostatic blood flow is discussed.

3.2.1. Moving laser beam.

At the start, the laser beam was situated in the center of the left side of the tissue model. The beam remained stationary for five seconds and then moved with either 0.5, 1 or 2 mm/sec to the right (comparable with the TULIP procedure). The results (axial and transversal planes) of the 0.5 mm/s speed are presented in figure 4.

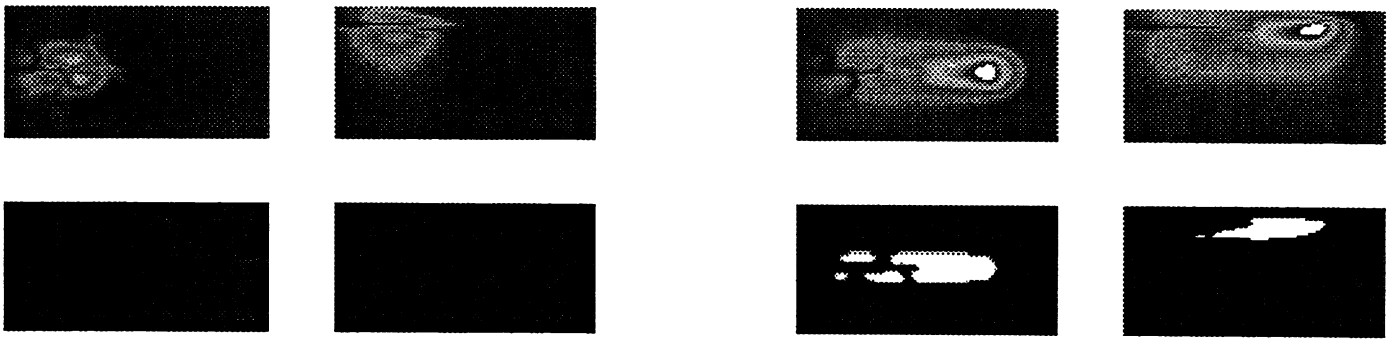

Figure 4. Results of the numerical model with a moving fiber. The top row presents the temperature distribution, the bottom row the tissue necrosis. The two left columns are the transversal (left) and axial (2nd from left) plane after 45 seconds (with blood vessels). The two right columns are the transversal (2nd from right) and the axial (right) plane after 135 seconds (without blood vessels).

The effect of blood flow can be appreciated if you compare the two frame columns on the left side (after 45 seconds) with the two on the right side (after 135 seconds). In the first case, the beam is above the middle of the vessel network, in the second case the beam is above non-perfused tissue. The heat penetration is somewhat larger, but the temperatures near the surface are much higher when no vessels are present. The associated area of necrosis is also bigger in the no-vessel situation. The effect of the different scanning speeds is mainly a difference in heat penetration. The heat penetrates deeper into the tissue with slower scanning speeds and so the associated depth of necrosis becomes larger. When considering the time evolution the delay between the rise in temperature and the grow of the tissue necrosis is striking. After the tissue has reached its maximum temperature and is cooling down already, the zone of necrosis starts to grow and will continue to grow, even until 60 seconds after the laser has been switched off. This is due to the time-integral relationship between necrosis and temperature (equation 1): the high temperature during laser irradiation may last too short to permanently damage the tissue at a particular place instantaneously. The relatively long period of cooling down, during which the temperature of the tissue is still elevated, may be enough to make the tissue become necrotic.

3.2.2. Static laser beam.

The frames in figure 5 (axial and transversal planes) show the temperature distribution, after 55 seconds, due to laser irradiation with a laser beam that remains at one location (comparable with some clinical protocols of side firing devices). The axial and transversal planes are at the same position as in the figures of the moving beam. The white color represents temperatures exceeding 100 degrees.

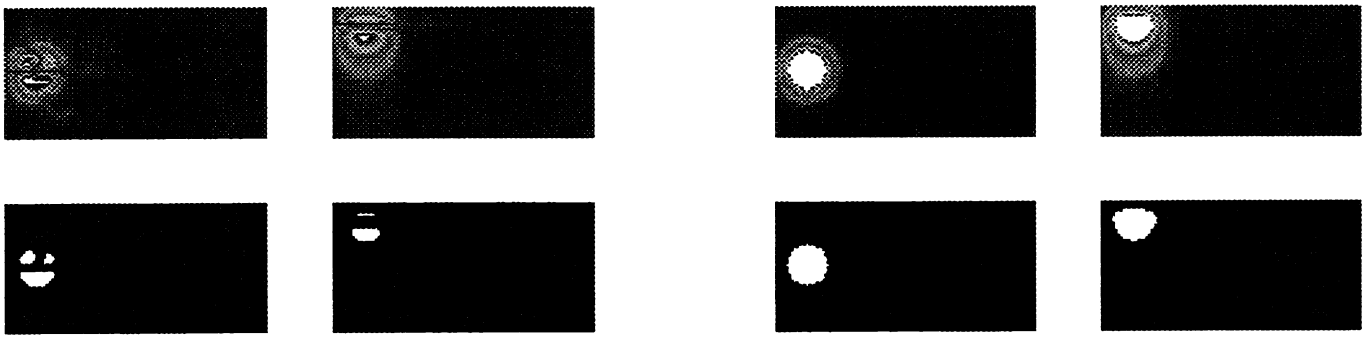

Figure 5. Results of the numerical model with a static fiber. The top row represents the temperature distribution, the bottom row the tissue necrosis. The two left columns are the transversal (left) and axial (2nd from left) plane of the model with blood vessels and the two right columns are the transversal (2nd from right) and the axial (right) plane of the model without blood vessels.

The blood vessels cool the tissue efficiently and limit the volume of necrosis. The temperatures near the surface reach higher values when no vessels are present. It should be realized that when the temperatures in the tissue are above 100 °C (the white color in the temperature frames), a chain of reactions takes place, e.g., popcorn and carbonization, leading to uncontrollable tissue ablation which is complex to model.

4. DISCUSSION

The numerical model shows that the blood vessels have a major influence on the temperature distribution and on the resulting long term tissue defect. The vessels act like a heat sink, which clamps the temperature and prevents the heat from penetrating deep into the tissue. Although the color of the tissue before treatment is never considered in pre-operative work-up, the model clearly shows that it will influence the volume of necrotic tissue.
During heating the optical properties, μ_a and μ'_s, of the tissue change. These changes influence the Monte Carlo simulation and result in a different light source (and associated heat source). The thermal parameters, k and c, which are used as an input for the temperature distribution calculation, will also change. The numerical model can be improved by feeding these changes back.
During laser irradiation of the tissue, the 'popcorn' effect might occur. Subsurface tissue water which is heated above ambient pressure boiling temperature, is prevented from escaping out of the tissue structure. At a sudden moment, the vapor pressure exceeds tissue resistance and vapor escapes explosively to the surface, causing the typical 'pop' sound[11]. Structural changes in the tissue induced by 'popcorn', carbonization and tissue vaporization, make the coagulation process of the prostate unpredictable and uncontrollable.

5. CONCLUSION

Modeling shows the influence of present blood vessels on the temperature distribution and on the tissue defect after a laser induced prostatectomy. The color of the tissue or the quantification of the blood flow through the prostate before a prostatectomy is an important parameter when evaluating the clinical results.

6. REFERENCES

1. R.A. Roth, R. Babayan, H.T. Aretz, "TULIP-transurethral ultrasound-guided laser-induced prostatectomy," J. Urol., Vol. 145, pp. 398A, 1991.
2. A.J. Costello, W.G. Bowsher, D.M. Bolton, K.G. Braslis, J. Burt, "Laser ablation of the prostate in patients with benign prostatic hypertrophy," *Br. J. Urol.*, Vol. 69, pp. 603-608, 1992.
3. E.M. Hardie, E.A. Stone, K.A. Spaulding, J.M. Cullen, "Subtotal canine prostatectomy with the neodymium:yttrium-garnet laser," *Vet. Surg.*, Vol. 19, pp. 348-355, 1990.
4. R.A. Roth, H.T. Aretz, "Transurethral Ultrasound-guided Laser-Induced Prostatectomy (TULIP): a canine feasibility study," *J. Urol.*, Vol. 146, pp. 1128-1135, 1991.
5. D.G. Assimos, D.L. McCullough, R.D. Woodruff, L.H. Harrison, L.J. Hart, W-J. Li, "Canine transurethral laser-induced prostatectomy," *J. Endourol.*, Vol. 5, pp. 145-149, 1991.
6. C.F.P. van Swol, R.M. Verdaasdonk, J. Mooibroek, T.A. Boon, "Clinical and physical evaluation of the TULIP system," Lasers in Urology, Gynecology and General Surgery, G.M. Watson, R.W. Steiner, D.E. Johnson (eds.), Vol. 1879, SPIE, Bellingham, 1993.
7. M. Keijzer, S.L. Jacques, S.A. Prahl, A.J. Welch, "Light distributions in artery tissue: Monte Carlo simulations for finite-diameter laser beams," Lasers Surg. Med., Vol. 9, pp. 148-154, 1989.
8. S.L. Jacques, S. Thomsen, J. Schwartz, M. Motamedi, S. Rastegar, I. Mannonen, "Comparing tissue optics and coagulation for a diode laser (805nm) versus the Nd:YAG laser (1064nm)," *Lasers Surg. Med.*, Suppl 4, pp. 5, 1992.
9. J. Mooibroek, J.J.W. Lagendijk, "A fast and simple algorithm for the calculation of convective heat transfer by large vessels in three dimensional inhomogeneous tissues," *IEEE Trans. Biomed. Eng.*, Vol. 38, pp. 490-501, 1991.
10. F.C. Henriques, "Studies of thermal injury," *Arch. Pathol.*, Vol. 43, pp. 489-502, 1947.
11. R.M. Verdaasdonk, C. Borst, M.J.C. van Gemert, "Explosive onset of continuous wave laser ablation," *Phys. Med. Biol.*, Vol. 35, pp. 1129-1144, 1990.